

Dynamics and structure of complex fluids from high frequency mechanical and optical rheometry

Norbert Willenbacher*, Claude Oelschlaeger

Institute of Mechanical Engineering and Mechanics, Research University of Karlsruhe [TH], 76131 Karlsruhe, Germany

Available online 24 March 2007

Abstract

High frequency rheometry here defined as measurement of dynamic shear moduli in the frequency range beyond that accessible by conventional rotational rheometry ($f > 10^2$ Hz) provides insight into microstructure and local dynamics of complex fluids. We review the mechanical devices as well as the optical and other microrheological techniques available today, discussing especially the frequency and modulus range the different methods cover. We also emphasise on the comparison between optical and mechanical methods and finally, on the microscopic structural and dynamic information extracted from high frequency rheology on complex fluids like polymers, surfactants, biomaterials and colloidal dispersions.

© 2007 Elsevier Ltd. All rights reserved.

Keywords: High frequency rheology; Microrheology; Viscoelasticity; Polymers; Surfactants; Colloidal dispersions

1. Introduction

The dynamics of complex fluids, such as colloidal suspensions, emulsions, gels or solutions of synthetic polymers, polyelectrolytes, surfactants or biopolymers and proteins extends across several orders of magnitude on the time ranging from microseconds to tens of seconds or even hours and days, thus reflecting the diversity of relaxation processes occurring in such fluids. High frequency rheology particularly provides insight into microstructure, interactions and local dynamics of complex fluids. This is of great interest both for pure and applied research. In the case of concentrated colloidal suspensions e.g. the high frequency modulus probes thermodynamic particle interactions and can be directly related to suspension stability. For polymer or surfactant solutions the hierarchical relaxation of structural elements results in characteristic scaling regimes for the high frequency moduli which can be related to microscopic features like chain stiffness, molecular architecture or solvent–polymer interactions. The location of the high frequency regime on an absolute scale of course

strongly depends on the characteristic features of the respective fluid and typically extends from 10 to 10^6 Hz. Conventional rotational rheometers are usually limited to frequencies $< 10^2$ Hz and for complex fluids time–temperature superposition is generally not suitable to extend this frequency range. In the past few years both mechanical and optical techniques have become increasingly available, covering the frequency range beyond 10^2 Hz. These techniques are now robust and accurate enough to study a wide variety of fluids from dilute (bio) polymer solutions to entangled networks and concentrated colloidal suspensions.

2. Mechanical devices

2.1. Piezo-driven shear and squeeze flow rheometer

Various piezo-driven oscillatory shear rheometers have been built to cover the frequency range from about 0.1 Hz to almost 10 kHz. Generation of flow as well as detection of sample response are handled by piezoelectric transducers. Frequency can be varied continuously and the applied strain amplitudes γ_0 are on the order of 10^{-4} – 10^{-3} . Moreover, the required sample volume is very small, typically < 100 μ l. Instruments operating in simple either linear [1] or torsional [2] shear flow are suitable for fluids with moduli $G^* > 10^2$ Pa.

* Corresponding author.

E-mail addresses: norbert.willenbacher@mvm.uni-karlsruhe.de
(N. Willenbacher), Claude.Oelschlaeger@mvm.uni-karlsruhe.de
(C. Oelschlaeger).

Piezo-rheometers operating in the squeeze flow mode have been introduced by Pechhold and co-workers [3] and Palierne [4]. For small deformations the complex squeeze stiffness K^* of such a set-up is related to the shear modulus G^* and compressibility κ^* of the fluid

$$\frac{1}{K^*} = \frac{2d^3}{3\pi R^4} \left(\frac{1}{G^*} + \frac{3R^2}{2d^2} \cdot \kappa^* \right) \quad (1)$$

where R and d are the gap radius and height, respectively. In principle, this allows for simultaneous determination of G^* and κ^* through variation of the gap height, but for dilute polymer or surfactant solutions the compressibility term is negligibly small. Shear moduli G^* down to 10^{-3} Pa are accessible. Recently, such devices have been used to study polymer and surfactant solutions, as well as colloidal suspensions and concentrated emulsions [3–5]. A linear shear flow rheometer has been placed into a magnetic field and combined with a light scattering device in order to study the structure and rheology of magnetic particles in polymeric matrices [6].

2.2. Torsional resonators

Torsional resonators provide access to the frequency range from about one to a few hundred kHz. Immersion of the resonator into a fluid results in a shift of the resonance frequency Δf and a broadening of the resonance curve ΔD compared to its behavior in air. The shear modulus G^* of the surrounding fluid is directly related to ΔD and Δf . First introduced about 60 years ago [7], various experimental designs have been employed [8,9] facilitating measurements at one or multiple frequencies. Resonators with different geometries (cylinder, tube, plate) as well as driving and detecting modes (piezo, electromagnetic, magnetostrictive) with high quality factors are available now [10], the required sample volume is typically >10 ml. Piezo-driven devices operate at strain amplitudes $\gamma_0 < 10^{-3}$. Such small strain amplitudes are mandatory to access the linear viscoelastic response regime e.g. in the case of concentrated colloidal suspensions. Moduli $G^* > 10$ Pa are accessible with the set-up used by Willenbacher and co-workers, but careful calibration is necessary [11]. Robust, electromagnetically driven resonators have been introduced recently by Romoscanu et al. [10,12]. Operating at $\gamma_0 > 10^{-2}$ reasonable results for Newtonian fluids and weakly viscoelastic polymer solutions with $G^* > 100$ Pa were obtained without calibration using only the mechanical specifications of the resonator set-up.

2.3. Ultrasonic shear rheometers

Piezoelectric crystal resonators oscillating in thickness-shear mode at frequencies in the MHz range are also used to obtain rheological information of complex fluids. Analogous to the torsional resonator technique described above, the mechanical impedance of the quartz crystal is coupled to the viscoelastic properties of the fluid in contact with its surface

[13]. The penetration depth δ of the shear wave is related to its frequency f as well as the density ρ and dynamic shear modulus $G^* = G' + iG''$ of the surrounding fluid:

$$\delta = \frac{|G^*|}{2\pi f} \sqrt{\frac{2}{\rho} \cdot \frac{1}{|G^*| - G'}} \quad (2)$$

Accordingly the penetration depth in the MHz range is often below $1 \mu\text{m}$ and the required sample volume is only a few microliters, but it has to be checked carefully, whether bulk properties are probed. Shear amplitudes are again around 10^{-3} and moduli $G^* > 10^4$ Pa are accessible. The technique has recently been used to study protein–protein interactions in concentrated protein solutions [14,15] or gelation in dairy products [16]. Alig et al. have set up an ultrasonic rheometer operating in the reflection mode. The shear modulus of a fluid film applied to the quartz block is inferred from the amplitude and the phase shift of the ultrasonic pulse reflected at the interface between quartz and fluid using special ultrasonic shearwave transmitters. This technique is less sensitive than the resonator method and moduli $10^6 \text{ Pa} < G^* < 10^9 \text{ Pa}$ are detectable, but it allows for characterization of thin fluid layers with one free surface. Recently, it has been used to study film formation from solutions and suspensions also in combination with spectroscopic methods [17].

2.4. Atomic force microscopy (AFM)

AFM is more and more used as a tool for nanorheology and -tribology, providing information about viscoelastic properties with high spatial resolution, stress–strain measurements are performed even with single polymer molecules [18]. The method requires only small sample volumes ($\ll 1 \mu\text{l}$), it is fast and thus especially suitable for high throughput screening. Naturally, AFM is a surface characterization method and it is widely used to characterize viscoelastic properties of polymer films or even biological cells [19]. Extracting absolute values for bulk rheological quantities of non-Newtonian fluids is still a challenge due to the complex and often poorly reproducible flow field around the cantilever tip. An AFM-based oscillatory strain microrheometer has been used to extract the dynamic tensile modulus E^* of polyacrylamide gels and biological cells based on a generalized Hertz model [20]. Analysis of the power spectral density of thermally-induced cantilever deflections is a different route to AFM-based dynamic mechanical spectroscopy and gives access to frequencies in the kHz range. So far, this has been used for viscosity measurements on simple liquids [21].

3. Optical techniques

Optical and other microrheological techniques including magnetic tweezers and AFM have rapidly developed within the last 10–15 years, consequently the state of the art has been summarized in various review articles [19,22–24,25]. We focus on the high frequency aspect here.

3.1. Diffusing wave spectroscopy (DWS) and video particle tracking

DWS as the extension of standard dynamic light scattering to turbid media is now increasingly used as a rheological tool [26–28]. Thermal motion of scattering objects results in transient intensity fluctuations. The corresponding transport of light related can be treated as a diffusion process and the decay of the autocorrelation function $g_2[\tau]$ can be expressed in terms of the ensemble average of the mean square particle displacement $\langle \Delta r^2[\tau] \rangle$, which in turn is related to the dynamic shear modulus G^* of the surrounding medium via a generalized Stokes Einstein relation

$$G^*(f) = \frac{kT}{\pi a \cdot i2\pi f \langle \Delta \tilde{r}^2(i2\pi f) \rangle} \quad (3)$$

with particle radius a , Boltzmann constant k , temperature T , and $\langle \Delta r^2(i2\pi f) \rangle$ being the Laplace transform of $\langle \Delta r^2[\tau] \rangle$. Scattering of objects inherently present in the fluid or added tracer particles can be analyzed, but the optical mean free path l^* must be determined accurately to obtain absolute values of G^* . Due to multiple scattering even small displacements of single particles of a few nanometers have a significant effect on the correlation function, accordingly linear viscoelastic properties of the surrounding fluid and short relaxation processes are probed. Shear moduli $10^{-1} \text{ Pa} < G^* < 10^4 \text{ Pa}$ are accessible in the frequency range from 10^{-1} to 10^5 Hz. Fast ensemble averaging is the advantage of DWS microrheology, but it does not provide rheological information on a local scale. Data analysis tacitly assumes, that the scattering particles move in a homogeneous, incompressible continuum without slip and it is not a priori clear whether this is valid for a given tracer/fluid system. Various examples have been reported showing good agreement between DWS microrheology and mechanical measurements at low frequencies [19,24], while in other cases substantial deviations are observed [29], which can also be used for systematic studies of the diffusion of colloidal particles in entangled polymer networks [30].

Video particle tracking (VPT) gives direct access to the mean square displacement of particles subject to thermal motion and is of particular importance, since it facilitates analysis of sample heterogeneities, even the local rheological properties of living cells can be studied with high spatial resolution [31]. Bulk rheological properties can be extracted even for heterogeneous samples using two-point microrheology [22,32]. In this approach cross-correlations of displacements of particles which are far apart (~ 10 – $100 \mu\text{m}$) are analyzed. This correlations are solely controlled by long range hydrodynamic interactions and thus independent of the local particle environment. The frequency range of particle tracking techniques is usually limited to 50 Hz according to standard video rates, but can in principle be extended to the kHz range using high speed cameras.

3.2. Optical and magnetic tweezers

Optical tweezers, also called optical traps, employ highly focused beams of light to capture and manipulate small

dielectric particles [23,24,25]. In the case of so-called ‘passive’ microrheology the power spectra of the thermal fluctuations of the trapped particles are analyzed using dispersion relations from linear response theory (c.f. AFM). This allows for a determination of G^* with high resolution and high band width. Shear moduli in the range between 10^{-2} Pa and 10^3 Pa are accessible in the frequency range from 10^{-1} to 10^5 Hz. The upper limit is determined by inertial effects, corresponding phenomena like vortex diffusion are still under investigation [33]. Particle trapping provides local information, two-point techniques (c.f. VPT) using particles in two well separated traps can be employed to extract bulk rheological properties [34,35].

Alternatively, optical tweezers can be used to apply a local stress by moving the laser beam, thus dragging the trapped particle through the surrounding fluid [‘active’ microrheology]. The resultant bead displacement is interpreted in terms of a viscoelastic fluid response [36]. The accessible frequency range is limited and this is no real high frequency technique, but since forces of about 10 pN (thermal force $\ll 1$ pN) can be applied, it can be either used to study fluids of higher viscosity or nonlinear rheological response.

Magnetic tweezers are another means of performing active microrheology. Stronger forces can be applied than with optical tweezers, but particle control is more sophisticated. Magnetic traps with various designs have been presented over the years and mostly they have been used to study biomaterials [19,25]. Magnetically driven probe particle motion is analyzed using videomicroscopy and usually these instruments operate at frequencies below 10 Hz. Keller et al. extended the frequency range to 40 Hz using a fast CCD camera and rapid imaging processing. This was sufficient to study the high frequency scaling regime of their F-actin solutions [37]. Fabry et al. further extended the frequency range to 10^3 Hz using heterodyne detection and studied the viscoelastic response of living cells [38].

4. High frequency dynamics and structure of complex fluids

4.1. Polymer solutions and gels

Optical techniques yield bulk rheological properties for polymer solutions as long as the characteristic length scales of the system are well below the size of the tracer particles and there are no specific interactions between the tracer and the constituents of the solution [19,22,24,25,39]. Accordingly DWS could be used to determine the high frequency scaling of G^* for semi-dilute solutions of linear polyethylene oxide [PEO] and a characteristic Rouse behavior ($G^* \sim \omega^{1/2}$) has been reported at high frequencies indicating hydrodynamic screening [40]. Similar scaling was found for charged polystyrene sulfonate combs in semi-dilute solution independent of the chain architecture [41], whereas Zimm-scaling ($G^* \sim \omega^{2/3}$) was observed for polyacrylamide gels at high frequencies irrespective of the degree of crosslinking [42]. In contrast, DWS microrheology of hydrophobically modified, end-capped PEO

solutions revealed a strong dependence on tracer particle size in the high frequency range, which was attributed to inhomogeneities of the associative network [43[•]].

4.2. Surfactant solutions

Entangled wormlike micellar surfactant solutions have been employed as model systems for comparison of optical and mechanical rheological techniques at a higher degree of fluid complexity. Special emphasis was on the high frequency scaling laws. Using cetylpyridinium chloride (CPyCl) as surfactant and sodium salicylate (NaSal) as a strongly binding counterion Schmidt and co-workers found excellent agreement between one- and two-point microrheology with optical tweezers [34,44]. Moreover, the optical data coincide very well with mechanical rheometry including squeeze flow in the whole frequency range up to 10 kHz [45^{••}]. The linear concentration dependence of G^* in the kHz range indicates that single chain relaxation processes dominate. A scaling exponent $\alpha=0.68\pm 0.1$ was extracted for the frequency dependence of the dynamic moduli [35,45^{••}], which is slightly lower than that expected for semiflexible chains. Willenbacher et al. [46^{••}] used a similar system to compare DWS tracer microrheology and mechanical rheometry including torsional resonance oscillation thus extending the mechanically accessed frequency range to 60 kHz. They also found good agreement between optical and mechanical rheometry in the whole frequency range. Moreover, the DWS data revealed a scaling exponent $\alpha=3/4$ for the frequency dependence of $G''-i\omega\eta_s$ beyond 10 kHz, which allowed for determination of the persistence length l_p of the wormlike micelles (Fig. 1). Consistent values of $l_p\approx 30$ nm were obtained both from the frequency at which transition from Zimm to $\omega^{3/4}$ -scaling was observed and from the absolute values of G'' in the latter regime according to [47].

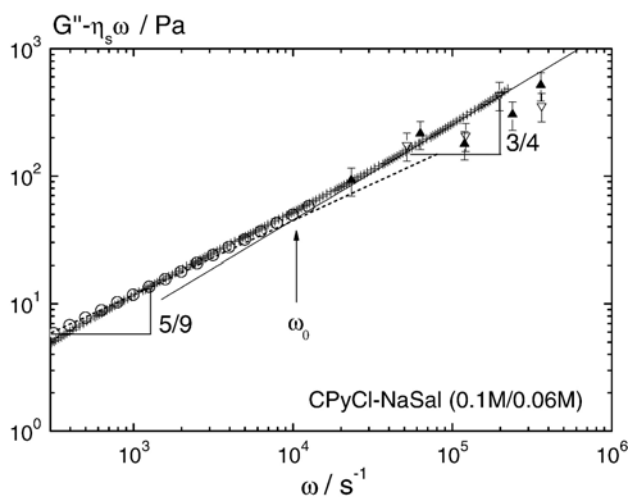


Fig. 1. Loss modulus $G''-i\omega\eta_s$ of an aqueous solution of 0.1 mol CPyCl/0.06 mol NaSal at 20 °C from oscillatory squeeze flow (○) and torsional resonance oscillation (▼,△) and DWS (+). Solid line: fit of Eq. (3) from [47] ($\omega^{3/4}$ -scaling) to the DWS data. Dashed line: $\omega^{5/9}$ -scaling fitted to the squeeze flow data. (redrawn from [46^{••}]).

4.3. Biomaterials

The rheological properties of biopolymers are of utmost interest due to their broad occurrence in all aspects of life science from food engineering to biotechnology and medical science. Generally, they exhibit a much more complexity than synthetic polymers.

The complex rheological behavior of starch and especially its gelation properties have been intensively studied in the past because of its wide application in food industry. DWS rheology revealed Rouse relaxation at high frequencies typical for flexible polymers [48] similar behavior was found in Xanthan. Aggrecan, a major constituent of articular cartilage, shows Zimm behavior [28] even in the kHz range, while CMC solutions exhibit a semi-flexible signature with a $G^* \sim \omega^{3/4}$ scaling [49].

Filamentous actin (F-actin), one of the constituents of the cytoskeleton is believed to be most important for mechanical strength and mobility of eukaryotic cells. Accordingly, it has been subject to numerous rheological and mechanical investigations during the past decade using mechanical rheometry, magnetic microrheology [19,50] and various optical techniques [31], revealing that different techniques provide different information which is not necessarily the bulk rheology. Nevertheless, the semi-flexible nature of the filaments expressing itself in the $G^* \sim \omega^{3/4}$ scaling has been clearly determined using DWS [51,52] and optical tweezers [19,34]. Due to the superior stiffness of the actin filaments ($l_p \approx 17 \mu\text{m}$), the high frequency regime sets in at $f > 1$ Hz for G'' and at $f > 10^3$ Hz for G' . More recently, this has been confirmed using optical trap two-point microrheology for physically entangled as well as chemically cross-linked F-actin solutions and gels [53^{••}]. Even the absolute values of the dynamic moduli could be predicted excellently using MacKintosh's statistical mechanical theory [47] with all parameters known from independent measurements (Fig. 2). Furthermore, a previously unknown relaxation due to axial tension propagation was observed which results in a stronger increase of G^* at high frequencies close to $G^* \sim \omega$ [53^{••}]. On the other hand, one-point microrheology underestimates the absolute value of G^* and provides the correct scaling only for G'' for F-actin, while good agreement is found between one- and two-point microrheology for fd-virus solutions also the characteristic length scales of both systems are similar to the size of the tracer particles used [54[•]]. In conclusion, high frequency rheology gives useful information about the stiffness and stress relaxation of biopolymers, but different macro- and microrheological techniques probe different length scales and have to be compared cautiously.

4.4. Colloidal dispersions and emulsions

Based on a theory for simple liquids theoretical expressions including hydrodynamic interactions have been derived relating the limiting high frequency modulus G'_∞ of concentrated dispersions to the colloidal interaction potential Ψ [55,56]. For aqueous colloidal dispersions the high frequency limit is typically reached beyond $f=1$ kHz. This concept generated robust

results not only for liquid [57] and ordered [58] charge stabilized dispersions, but also for sterically stabilized systems [59]. Recently, Fritz et al. [60] successfully applied these concepts to the commercially significant class of electrosterically stabilized polymer dispersions directly revealing under which conditions of pH and ionic strength either charge or steric interactions were dominating. A frequency independent value G'_{∞} is only found when electrostatic interactions dominate, “hairy” particle surfaces give rise to a weak power-law dependence $G' \sim \omega^{\alpha}$ with $\alpha \approx 0.25–0.35$, presumably due to the relaxation of polymer chains in the “hairy” stabilizing layer [13] (Fig. 3). In another study on hard sphere suspensions an exponent $\alpha = 0.59 \pm 0.1$ was found [61] and in line with earlier theoretical predictions [62], this can be attributed to hydrodynamic interactions when particles closely approach. Furthermore, Fritz et al. [60] have demonstrated, that the high

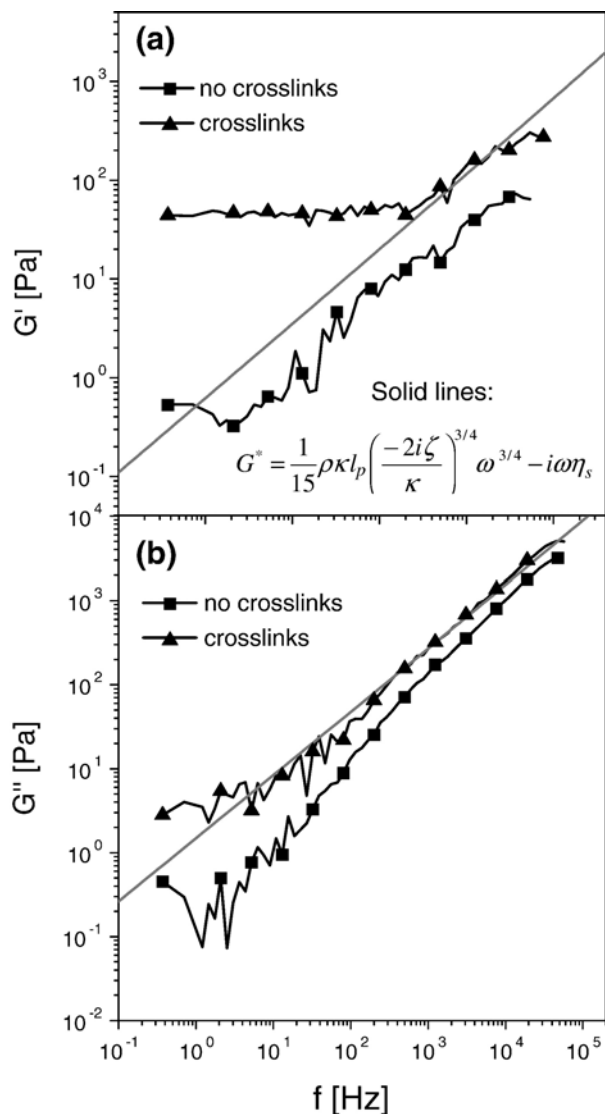


Fig. 2. (a) Storage modulus $G'(\omega)$ and (b) (absolute) loss modulus $G''(\omega)$ of 1 mg/ml solutions of F-actin filaments without (squares) and with (triangles) cross-linking plotted against frequency $f = \omega/2\pi$. Solid lines: theory, Eq. (3) from [47]. Inset: scaled loss modulus $G_s''(\omega) = -[G''(\omega) + i\omega\eta]/(c_A \cdot \omega^{3/4})$. (redrawn from [53]).

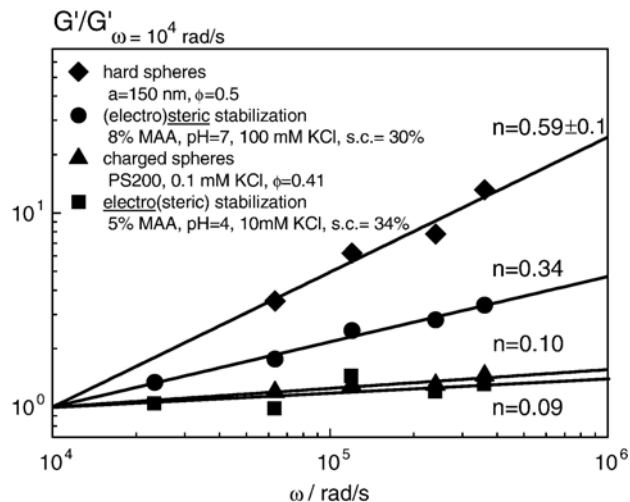


Fig. 3. Frequency dependence of G' in the kHz range. Concentrated colloidal dispersions with different modes of stabilization exhibit characteristic scaling exponents. (redrawn from [11]).

frequency viscosity of “hairy” particle suspensions deviates substantially from that of hard or charged sphere systems at effective volume fractions $\phi^{\text{eff}} > 0.5$, revealing the drainage of the hairy layer by the solvent. Their data could be quantitatively analyzed using a permeable shell model [55].

Still little is known about the high frequency rheological behavior of emulsions. A preliminary study on low viscosity o/w-emulsions was done by Romoscanu et al. [63] including data in the kHz range, where elasticity is expected to occur due to droplet deformation. Their results were consistent with the well-known Palierne model. A broad distribution of relaxation times and a corresponding $\omega^{1/2}$ scaling has been observed for monodisperse emulsions at concentrations beyond the maximum packing fraction [4] and has been attributed to the existence of randomly oriented slip planes with relaxation times depending on their relative orientation relative to the direction of shear. Mechanical squeeze flow data agree very well with earlier DWS measurements [64].

5. Conclusions

Robust and reliable mechanical devices are now available to characterize the linear viscoelastic properties of complex fluids cover the frequency range up to 100 kHz. They are complemented by optical (and also magnetic) microrheological tools, which are extremely sensitive and require only very small sample volumes. Specific interactions of tracer particles with their particular microenvironment have to be considered carefully, when comparing with results from bulk mechanical measurements. But on the other hand, deviations between bulk and microrheology can also be utilized to extract information about local rheological features of inhomogeneous fluids on a micron scale. This will be especially useful in the strongly growing field of bio- and cellphysics. Optical tweezers and DWS in combination with refined theories about the transition from ballistic to Brownian motion will provide new insight into fluid dynamic phenomena as well as previously hardly accessible relaxation modes of complex

fluids even in the MHz range. DWS has developed as a versatile tool for systematic studies not only of the stiffness of surfactant micelles but also of other semi-flexible objects like carbon nanotubes or self-assembling planar polymers. The high frequency rheology of suspensions of repulsive particles is quite well understood, but still little is known about attractive particle suspensions and emulsions. Exploration of these areas will surely reveal new insight into the structure and stability of these systems, especially about the relaxation modes of polymers adsorbed at interfaces.

References and recommended reading [12]

- [1] Gallani JL, Hilliou L, Martinoty P, Doublet F, Mauzac M. Mechanical behavior of side-chain liquid crystalline networks. *J Phys II* 1996;6:443.
- [2] Kirschenmann L, Pechhold W. Piezoelectric Rotary Vibrator (PRV) — a new oscillating rheometer for linear viscoelasticity. *Rheol Acta* 2002;41:362–8.
- [3] Crassous JJ, Régisser R, Ballauff M, Willenbacher N. Characterization of the viscoelastic behavior of complex fluids using the piezoelectric axial vibrator. *J Rheol* 2005;49:851–63. Kirschenmann, L. PhD Thesis, Institut für Dynamische Materialprüfung, University of Ulm, 2003.
- [4] Hebraud P, Lequeux F, Paliere JF. Role of permeation in the linear viscoelastic response of concentrated emulsions. *Langmuir* 2000;16:8296.
- [5] Constantin D, Paliere JF, Freyssingas E, Oswald P. High-frequency rheological behaviour of a multiconnected lyotropic phase. *Europhys Lett* 2002;58(2):236–42. At high surfactant concentrations the entanglement concept breaks down, correspondingly the terminal relaxation time drops to a few μs . A mechanistic model is proposed to rationalize stress relaxation assuming local hexagonal order induced by micelle–micelle interactions.
- [6] Auernhammer GK, Collin D, Martinoty P. High-frequency rheological behaviour of a multiconnected lyotropic phase. *J Chem Phys* 2006;124:1–10.
- [7] Mason WP. Measurement of the viscosity and shear elasticity of liquids by means of a torsionally vibrating crystal. *Trans A S M E* 1949;69:359–70.
- [8] Schrag JL, Johnson RM. Application of the Birnboim multiple lumped resonator principle to viscoelastic measurements of dilute macromolar solutions. *Rev Sci Instrum* 1971;42:224–32.
- [9] Blom C, Mellema J. Torsion pendula with electromagnetic drive and detection system for measuring the complex shear modulus of liquids in the frequency range 80–2500 Hz. *Rheol Acta* 1984;23:98–105.
- [10] Romoscanu A, Sayir MB, Häusler K, Servais C. High frequency probe for the measurement of the complex viscosity of liquids. *Meas Sci Technol* 2003;14:451–62.
- [11] Fritz G, Pechhold W, Willenbacher N, Wagner NJ. Characterizing complex fluids with high frequency rheology using torsional resonators at multiple frequencies. *J Rheol* 2003;47:303–19. Characteristic scaling exponents are observed for G' of concentrated colloidal dispersions in the kHz range. Only for charge stabilized systems G'_{∞} is essentially independent of frequency. The frequency dependence of G' can be attributed to hydrodynamic or polymer relaxation phenomena depending on the dominating type of colloidal interactions (see Fig. 3 and [60*,61]).
- [12] Romoscanu AI, Sayir MB, Häusler K, Burbidge AS. High frequency parallel plate probe for the measurement of the complex viscosity of liquids. *Rheol Acta* 2003;42:462–76.
- [13] Bandey HL, Martin SJ, Cemosek RW, Hillman AR. Modeling the responses of TSN resonators under various loading conditions. *Anal Chem* 1999;71:2205–14.
- [14] Saluja A, Badkar AV, Zeng DL, Nema S, Kalonia DS. Application of high-frequency rheology measurements for analyzing protein–protein interactions in high protein concentration solutions using a model monoclonal antibody (IgG2). *J Pharm Sci* 2006;95(9):1967–83.
- [15] Saluja A, Kalonia DS. Application of ultrasonic shear rheometer to characterize rheological properties of high protein concentration solutions at microliter volume. *J Pharm Sci* 2005;94(6):1161–8.
- [16] Kudryashov ED, Hunt NT, Arikainen EO, Buckin VA. Monitoring of acidified milk gel formation by ultrasonic shear wave measurements. High-frequency viscoelastic moduli of milk and acidified milk gel. *J Dairy Sci* 2001;84(2):375–88. Gelation of casein particles is studied using ultrasonic and low frequency rheological techniques. Different mechanisms of stress relaxation in the casein network are identified according to their contribution to the high and low frequency moduli. In the MHz range shear and compression moduli are found to be of the same order of magnitude for such systems.
- [17] Alig I, Steeman PAM, Lellinger D, Dias AA, Wienke D. Polymerization and network formation of UV-curable materials monitored by hyphenated real-time ultrasound reflectometry and near-infrared spectroscopy (RT-US/NIRS). *Prog Org Coat* 2006;55(2):88–96.
- [18] Nakajima K. Polymer nanoscience revealed by atomic force microscopy. *Novel Strategies for Fundamental Innovation in Polymer Science*; 2005. p. 97–121. Garcia R, Perez R. Dynamic atomic force microscopy methods. *Sci Rep* 2005;47(6–8):197–301.
- [19] MacKintosh FC, Schmidt CF. Microrheology. *Curr Opin Colloid Interface Sci* 1999;4(4):300–7.
- [20] Mahaffy RE, Shih CK, MacKintosh FC, Käs J. Scanning probe-based frequency-dependent microrheology of polymer gels and biological cells. *Phys Rev Lett* 2000;85:880.
- [21] Boskovic S, Chon JWM, Mulvaney P, Sader JE. Rheological measurements using microcantilevers. *J Rheol* 2002;46:891.
- [22] Mukhopadhyay A, Granick S. Micro- and nanorheology. *Curr Opin Colloid Interface Sci* 2001;6(5–6):423–9.
- [23] Furst EM. Applications of laser tweezers in complex fluid rheology. *Curr Opin Colloid Interface Sci* 2005;10(1–2):79–86.
- [24] Gardel ML, Valentine MT, Weitz DA. In: Breuer K, editor. *Microscale diagnostic techniques*. Springer Verlag; 2005. Excellent review of optical and other microrheological techniques. Technical principles and specifications, theoretical foundations and physical limits are outlined. Instructive examples and essential applications are presented.
- [25] Waigh TA. Microrheology of complex fluids. *Rep Prog Phys* 2005;68:685–742.
- [26] Scheffold F, Romer S, Cardinaux F, Bissig H, Stradner A, Rojas-Ochoa LF, et al. New trends in optical microrheology of complex fluids and gels. *Prog Colloid & Polym Sci* 2004;123:141–6.
- [27] Scheffold F, Cardinaux F, Schurtenberger P. Some recent advances in DWS based optical microrheology. *Abstracts of Papers, 230th ACS National Meeting*, Washington, DC, United States; Aug. 28–Sept. 1, 2005.
- [28] Papagiannopoulos A, Waigh TA, Hardingham T, Heinrich M. Solution structure and dynamics of cartilage aggrecan. *Biomacromolecules* 2006;7(7):2162–72.
- [29] Gardel ML, Valentine MT, Crocker JC, Bausch AR, Weitz DA. Microrheology of entangled F-actin solutions. *Phys Rev Lett* 2003;91: 158302.
- [30] Huh JY, Furst EM. Colloid dynamics in semiflexible polymer solutions. *Phys Rev E* 2006;74:031802. DWS is used to study the diffusion of particles in dilute and entangled F-actin solutions. Filament length as well as particle size are varied systematically. Particle dynamics suggests the formation of a local depletion layer in entangled solutions. The layer thickness correlates well with non-locality length of entropic repulsion obtained from PRISM theory.
- [31] Daniels BR, Masi BC, Wirtz D. Probing single-cell micromechanics in vivo: the microrheology of *C. elegans* developing embryos. *Biophys J* 2006;90(12):4712–9. Tseng Y, Kole TK, Lee S-HJ, Wirtz D. Local dynamics and viscoelastic properties of cell biological systems. *Curr Opin Colloid Interface Sci* 2006;7(3–4):210–7.
- [32] Crocker JC, Valentine MT, Weeks ER, Gislis T, Kaplan PD, Yodh AG, et al. Two-point microrheology of inhomogeneous soft materials. *Phys Rev Lett* 2000;85(4):888–91. Levine AJ, Lubensky TC. One- and two-particle microrheology. *Phys Rev Lett* 2000;85:1774–7.

• Of special interest.

•• Of outstanding interest.

- [33] Atakhorrami M, Koenderink GH, Schmidt CF, MacKintosh FC. Short-time inertial response of viscoelastic fluids: observation of vortex propagation. *Phys Rev Lett* 2005;95(20):208302. Fluid inertia as a limitation of microrheology at high frequencies is explored. Two optically trapped beads are used to investigate vortex propagation on a μs time scale. For viscoelastic fluids, this propagation is shown to be faster than diffusive and the displacement correlations reflect the frequency-dependent shear modulus of the medium.
- [34] Gittes F, Schnurr B, Olmsted PD, MacKintosh FC, Schmidt CF. Microscopic viscoelasticity: shear moduli of soft materials determined from thermal fluctuations. *Phys Rev Lett* 1997;79:3286.
- [35] Atakhorrami M, Schmidt CF. High-bandwidth one and two-particle microrheology in solutions of wormlike micelles. *Rheol Acta* 2006;45:449–56.
- [36] Raghu A, Ananthamurthy S. Construction of an optical tweezer for nanometer scale rheology. *J Phys* 2005;65(4):699–705.
- [37] Keller M, Schilling J, Sackmann E. Oscillatory magnetic bead rheometer for complex fluid microrheometry. *Rev Sci Instrum* 2001;72(9):3626–34.
- [38] Fabry B, Maksym GN, Butler JP, Glogauer M, Navajas D, Fredberg JJ. Scaling the microrheology of living cells. *Phys Rev Lett* 2001;87(14):148102.
- [39] Solomon MJ, Lu Q. Rheology and dynamics of particles in viscoelastic media. *Curr Opin Colloid Interface Sci* 2001;6(5–6):430–7.
- [40] Dasgupta BR, Shang-You T, Crocker JC, Frisken BJ, Weitz DA. Microrheology of polyethylene oxide using diffusing wave spectroscopy and single scattering. *Phys Rev E* 2002;65:051505.
- [41] Mason TG, Ganesan K, van Zanten JH, Wirtz D, Kuo SC. Particle tracking microrheology of complex fluids. *Phys Rev Lett* 2002;79(17):3282–5.
- [42] Papagiannopoulos A, Fernyhough CM, Waigh TA. The microrheology of polystyrene sulfonate combs in aqueous solution. *J Chem Phys* 2005;123(21):214904/1–214904/10.
- [43] Dasgupta BR, Weitz DA. Microrheology of cross-linked polyacrylamide networks. *Phys Rev E* 2005;71:021504.
- [44] Lu Q, Solomon MJ. Probe size effects on the microrheology of associating polymer solutions. *Phys Rev E* 2002;66(6-1):061504/1–061504/11. The limitations of DWS microrheology are demonstrated for solutions of hydrophobically modified, end-capped polyethylene oxide (PEO). Results strongly depend on particle size but not on particle surface properties and the generalized Stokes–Einstein equation breaks down at polymer concentrations $>0.5\%$. This is in contrast to observations on linear PEO (c.f. [40]) and most probably due to structural inhomogeneity of the solution.
- [45] Buchanan M, Atakhorrami M, Palieme JF, Schmidt CF. Comparing macrorheology and one- and two-point microrheology in wormlike micelle solutions. *Macromolecules* 2005;38:8840–4.
- [46] Buchanan M, Atakhorrami M, Palieme JF, MacKintosh FC, Schmidt CF. High-frequency microrheology of wormlike micelles. *Phys Rev E* 2005;72:011504. Good agreement between dynamic shear moduli from one-point, two-point microrheology and mechanical rheometry is demonstrated here for the first time in the frequency range up to 10 kHz using wormlike micellar solutions as model system.
- [47] Willenbacher N, Scheffold F, Oelschlaeger C, Schopferer M, Cardinaux F, Fischer P. Broad Bandwidth Optical and Mechanical Rheometry of Wormlike Micelle Solutions. *Phys Rev Lett* submitted for publication. Dynamic shear moduli from DWS and various mechanical rheometrical techniques are shown to agree very well for a wormlike micellar solution in the frequency range up to 100 kHz. First rheological report of $\omega^{3/4}$ -scaling for wormlike micelles. The shortest Rouse time (determined as cross-over from $\omega^{5/9}$ to $\omega^{3/4}$ -scaling) and the absolute values of G'' yield consistent values for the persistence length $l_p \approx 35$ nm for this system (see Fig. 1).
- [48] Morse DC. Viscoelasticity of tightly entangled solutions of semiflexible polymers. *Phys Rev E* 1998;58:R1237.
- [49] Heinemann C, Cardinaux F, Scheffold F, Schurtenberger P, Escher F, Conde-Petit B. Tracer microrheology of g-dodecalactone induced gelation of aqueous starch dispersions. *Carbohydr Polym* 2004;55(2):155–61.
- [50] Pashkovski EE, Masters JG, Mehreteab A. Viscoelastic scaling of colloidal gels in polymer solutions. *Langmuir* 2003;19(9):3589–95.
- [51] Schmidt CF, Hinner B, Sackmann E. Microrheometry underestimates the values of the viscoelastic moduli in measurements on F-actin solutions compared to macrorheometry. *Phys Rev E* 2000;61(5 Pt B):5646–53.
- [52] Mason TG, Gisler T, Kroy K, Frey E, Weitz DA. Rheology of F-actin solutions determined from thermally driven tracer motion. *J Rheol* 2000;44(4):917–28.
- [53] Palmer A, Mason TG, Xu J, Kuo SC, Wirtz D. Diffusing wave spectroscopy microrheology of actin filament networks. *Biophys J* 1999;76(2):1063–71.
- [54] Koenderink GH, Atakhorrami M, MacKintosh FC, Schmidt CF. High-frequency stress relaxation in semiflexible polymer solutions and networks. *Phys Rev Lett* 2006;96:138307. The absolute values of the dynamic shear moduli of F-actin solutions are shown to be well predicted by the statistical mechanical theories with all relevant parameters are inferred from independent experiments (see Fig. 2). First experimental evidence for rapid stress relaxation due to tension propagation along the filament axis, resulting in a strong increase of G^* at high frequencies.
- [55] Atakhorrami M, Addas KM, Buchanan M, Koenderink GH, MacKintosh FC, Tang JX, Schmidt CF. Molecular Mechanics of Cytoskeletal Components. *Mechanics of the 21st century*; 2005. p. 355–64, doi:10.1007/1-4020-3559-4. Summarizes the results and characteristic differences between one- and two-point microrheology for model systems with different inherent length scales (wormlike micelles, F-actin, Fd-virus).
- [56] Elliot SL, Russel WB. High frequency shear modulus of polymerically stabilized colloids. *J Rheol* 1998;42:361.
- [57] Nommensen PA, Duits MHG, van den Ende D, Mellema J. Elastic modulus at high frequency of polymerically stabilized suspensions. *Langmuir* 2000;16:1902.
- [58] Horn FM, Richtering W, Bergholtz J, Willenbacher N, Wagner NJ. Hydrodynamic and colloidal interactions in concentrated charge-stabilized polymer dispersions. *J Colloid Interface Sci* 2000;225:166.
- [59] Buscall R, Goodwin JW, Hawkins MW, Ottewill RH. Viscoelastic properties of concentrated latices. Part 1. Methods of examination. *J Chem Soc Faraday Trans I* 1982;78:2889.
- [60] Deike I, Ballauff M, Willenbacher N, Weiss A. Rheology of thermo-sensitive latex particles including the high-frequency limit. *J Rheol* 2001;45:709.
- [61] Fritz G, Schädler V, Willenbacher N, Wagner NJ. Electrosteric stabilization of colloidal dispersions. *Langmuir* 2002;18:6381–90. The dominating effect of steric repulsion in technically relevant electro-sterically stabilized polymer dispersions is quantitatively deduced from a systematic analysis of the high frequency modulus based on well-established statistical mechanical relations between the modulus, colloidal interactions and microstructure.
- [62] Fritz G, Maranzano BJ, Wagner NJ, Willenbacher N. High frequency rheology of hard sphere colloidal dispersions measured with a torsional resonator. *J Non-Newton Fluid Mech* 2002;102:149–56.
- [63] Lionberger RA, Russel WB. High frequency modulus of hard sphere colloids. *J Rheol* 1994;38:1885.
- [64] Romoscanu AI, Sayir MB, Hausler K, Burbidge AS. Rheological behavior of low-viscous emulsions and interpretation with a theoretical model. *Colloids Surf A Physicochem Eng Asp* 2003;223(1–3):113–33.
- [65] Liu AJ, Ramaswamy S, Mason TG, Gang H, Weitz DA. Anomalous viscous loss in emulsions. *Phys Rev Lett* 1994;76:3017.